Mn(II)-Based Lipidic Nanovesicles as High-Efficiency MRI Probes

Mn(II)-based lipidic nanovesicles as high efficiency MRI probes

Gilberto Mulas,[‡] *Gabriele A. Rolla*,[†] *Carlos F.G.C. Geraldes*,[ʃ&] *Lucas W.E. Starmans*,[#] *Mauro Botta*,[†] *Enzo Terreno*,[‡*] *Lorenzo Tei*[†*]

[‡] Centro di Imaging Molecolare e Preclinico, Dipartimento di Biotecnologie Molecolari e Scienze della Salute, Università di Torino, Via Nizza 52, 10126 Torino, Italy

[†] Dipartimento di Scienze ed Innovazione Tecnologica, Università del Piemonte Orientale, Viale T. Michel 11, Alessandria, 15121, Italy

[ʃ] Department of Life Sciences and Coimbra Chemistry Center, Faculty of Science and Technology, University of Coimbra, 3000-393 Coimbra, Portugal

[&] CIBIT/ICNAS - Instituto de Ciências Nucleares Aplicadas à Saúde. Pólo das Ciências da Saúde, Azinhaga de Santa Comba, 3000-548 Coimbra, Portugal

[#] Biomedical Engineering, Eindhoven University of Technology, 5656, AE Eindhoven, The Netherlands

KEYWORDS

Manganese, amphiphilic chelating ligands, nanoparticles, liposomes, relaxometry.

ABSTRACT

Although nowadays there is a renewed and growing interest on Mn-based contrast agents, there are only few studies dealing with Mn-based lipophilic nanoparticles and on the strategies of their relaxivity optimization. Thus, three paramagnetic Mn(II) complexes based on amphiphilic derivatives of EDTA and 1,4-DO2A were used for the preparation of lipidic nanoparticles. The structural properties (length and position on the molecule of aliphatic chains) of amphiphilic Mn(II)-complexes control size and morphology of phospholipid-based self-assembling nanoaggregates, thus forming either vesicular liposomes, non-vesicular bicelles or a mixture of both. Consequently, hydrophilic Gd-based contrast agents or fluorescent dyes can, or cannot, be entrapped in the aqueous core of the nanoaggregate. This behaviour was studied in detail by using also diamagnetic amphiphilic Zn(II) analogues, entrapping gadoteridol in the aqueous core (where present) and collecting cryo-TEM images for structural elucidation. Furthermore, a detailed ^{1}H NMR relaxometric analysis was carried out on all systems highlighting an enhanced relaxivity with respect to monomeric analogues. In case of homogeneous systems, the data were also fitted to obtain the relaxometric parameters for comparison with literature data. Finally, this work allowed to understand how to control the formation of different type of nanovesicles (liposomes, bicelles, micelles) that will provide different *in vivo* biodistribution and how to optimize their MRI contrast.

INTRODUCTION

Magnetic Resonance Imaging (MRI) has proven to be an excellent tool to access diagnostic information readily and almost non-invasively, routinely used in the medical practice in the last thirty years.[1] During this period, the technique has evolved tremendously, and now several

diagnostic imaging applications are in the pipeline for clinical translation. Besides diagnosis, MRI is one of the techniques of election in the field of theranostics, where its unique characteristics are exploited to offer a valuable *in vivo* imaging support to pharmacological therapy and surgery intervention.[2] One typical theranostic protocol is to monitor the *in vivo* biodistribution of a drug, with particular emphasis to the accumulation in the site where the drug has to exert its therapeutic effect.[3] This task is commonly pursued by designing injectable systems in which the drug and the imaging reporter may have the same biodistribution because they share a given carrier. Among the clinically approved carriers, liposomes are certainly among the most commonly used as witnessed by the high number of theranostic studies that have involved these soft nanoparticles.[4]

When the aim of the theranostic protocol is to monitor the drug biodistribution *in vivo*, the imaging probe (as well as the drug) needs to be stably loaded into the carrier. Furthermore, to overcome the intrinsically low sensitivity of MRI, the probe should have an increased ability to alter the contrast in the region where it distributes. These two requirements can be successfully addressed by incorporating amphiphilic MRI contrast agents (CAs) in the bilayered membrane of liposomes.[5-8] The MRI CAs that are approved for clinical use are paramagnetic complexes of the lanthanide Gd(III) ion, and the theranostic potential of Gd-loaded lipid-based nanoparticles, such as liposomes, has been already demonstrated at preclinical level.[8-11]

However, the recent concerns about the potential risks associated with the use of Gd(III)-chelates,[12-13] prompted many researchers working in this field to explore alternative agents. Paramagnetic Mn(II) complexes were the first candidates due to the high biocompatibility and importance for life of the Mn(II) ion.[14-19] In principle, Mn(II)-complexes are less efficient than Gd(III)-analogues in generating MRI contrast primarily due to the lower number of unpaired electrons (5 d electrons *vs*. 7 f electrons). The efficiency of a paramagnetic complex is measured

as relaxivity, r_1, which represents the paramagnetic contribution to the longitudinal water proton relaxation rate enhancement per millimolar concentration of paramagnetic metal, at a given temperature and magnetic field strength. In the last decade, Mn(II) complexes with high thermodynamic stability, good kinetic inertness, and improved relaxivity have been extensively studied and stable chelates where the metal center is coordinated to one water molecule (q = 1) have been developed.[14, 15]

Though liposomes loaded with free Mn(II) ions have been already considered for theranostic applications,[20,21] only two studies dealing with amphiphilic Mn(II) complexes incorporated in the vesicles bilayer as MRI contrast agents were published up to 1997.[22,23] In the first study, the amphiphilic Mn(II) complexes of diethylenetriaminepentaacetic acid (DTPA) bis-amides of the octadecylesters of tyrosine or phenylalanine (MnDTPA-BTO and MnDTPA-BPO, respectively) were inserted into the membrane of lecithin-cholesterol liposomal vesicles and their r_1 relaxivity was measured at 80 MHz.[22] In the second work, published almost 30 years ago, the relaxometric properties of small unilamellar liposomes incorporating the Mn(II) complex of a DTPA-based ligand conjugated with two lipophilic stearic acid moieties *via* amide bonds were investigated *in vivo* on healthy rats and dogs.[23] The authors emphasized the poor *in vivo* stability of the investigated Mn(II)-chelates that released into liver and spleen a significant fraction (*ca*. 40%) of the injected Mn(II) ions. This negative result can be attributed to the choice of an unsuitable ligand for Mn(II), due to the presence of the two less basic (and weakly coordinating) carboxyamido moieties and a number of donor atoms (8) higher than the typical coordination number of Mn(II) (6/7).

On this basis, we have recently reported a series of Mn(II) complexes with EDTA- and 1,4-DO2A-like ligands (1,4-DO2A = 1,4,7,10-tetraazacyclododecane-1,4-diacetic acid) embodying two

aliphatic chains on the ethylene backbone in the case of EDTA (HCDTA ligand, Scheme 1) and on the free secondary amines of 1,4-DO2A in the 7,10 positions (DD-DO2A and DH-DO2A ligands, with C_{12} or C_{16} chains, respectively, Scheme 1).[24] The resulting amphiphilic Mn-complexes are able to self-aggregate in micellar structures in water and to interact strongly with human serum albumin (HSA), thus providing a strong relaxivity enhancement with respect to the monomeric chelates. It should be underlined that the parent $Mn(EDTA)^{2-}$ complex is an heptadentate Mn(II) complex featuring one metal-coordinated water molecule (q = 1) and a good relaxivity value (3.3 $s^{-1}mM^{-1}$ at 298 K and 0.47 T). However, the thermodynamic stability and, in particular, the kinetic inertness of this coordination cage, measured by transmetallation reactions with Zn(II) or Cu(II) in the pH range 3-6, (half-life at pH 7.4, $t_{1/2}$ = 0.076 h), are not high enough for *in vivo* applications.[25] Contrarily, the macrocycle Mn(1,4-DO2A) complex showed a good stability in physiological conditions either from a thermodynamic or a kinetic point of view ($t_{1/2}$ = 48.3 h at pH 7.4, measured as described above).[26] However, this chelate is in equilibrium between two forms with different hydration states (q = 1 / q = 0 in 87:13 ratio) resulting in a relaxivity lower than for $Mn(EDTA)^{2-}$ (2.1 $mM^{-1}s^{-1}$ at 298 K and 0.47 T).[27] The presence of two aliphatic chains renders these chelates amphiphilic and reduces their rotational dynamics when bound to HSA, self-assembled in micelles or incorporated in nanoparticles. The restricted rotational motion favors a remarkable relaxivity increase, especially in the 0.5-1.5 T range of magnetic field strengths.[7,28] Such a behavior was first reported for Gd(III) complexes embedded in the membrane of liposomes, which showed a 100% increase of r_1 for the bis-alkylated chelate with respect to the Gd(III) complex having a single C_{12} alkyl chain (at 1.5 T and 298 K).[29, 30]

The aim of this study is to assess the physico-chemical and relaxometric properties of liposomes incorporating the amphiphilic Mn(II) complexes mentioned above and evaluate their potential as novel nanoplatforms for MRI-based theranostic applications.

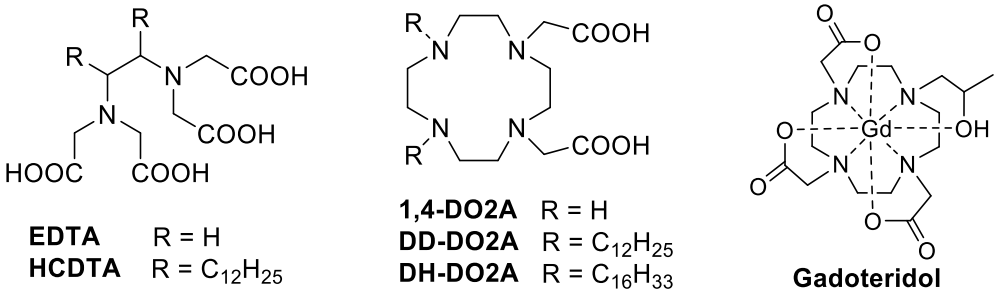

Scheme 1. Amphiphilic ligands used for the synthesis of Mn(II) and Zn(II) complexes and Gadoteridol.

Experimental section

Chemicals. 1,2-dipalmitoylphosphtidylcholine (DPPC) and 1,2-distearoyl-sn-glycero-3-phosphoethanolamine-*N*-[methoxy(polyethylene glycol)-2000] (DSPE-PEG2000) were purchased from Avanti Polar Lipids (Alabaster, AL, USA). All the other chemicals were purchased from Sigma–Aldrich Co and used without further purification. HCDTA, DD-DO2A and DH-DO2A ligands were synthesized as reported previously.[24]

Synthesis of the metal complexes. The ligands HCDTA, DD-DO2A and DH-DO2A were dissolved in water (10 mmol), and the pH of the solution was adjusted to 6.5. A solution of $Mn(NO_3)_2$ was added stepwise to the former solution adjusting the pH to 6.5 after each addition. The longitudinal relaxation rate of water protons was measured after each addition (0.47 T, 298 K) and the data were plotted versus the total concentration of Mn(II) added. A linear dependence of the longitudinal relaxation rate was observed, which indicated the formation of the metal complex. In addition, the slope of the line gave the millimolar relaxivity of the paramagnetic

species. The exact concentration of the Mn(II) ions in the solutions was measured via the bulk magnetic susceptibility (BMS) shift method (Mn(II) μ_{eff} = 5.94 μB).[31] In the case of the Zn(II) complexes, the metal salt dissolved in water was added in equimolar amount to the ligand solutions and the pH adjusted to 6.5. After 2 h reaction, the solution was lyophilized to obtain a white solid in quantitative yield. $[Zn(HCDTA)]^{2-}$: m/z (ES-) 691.0 $[M + H]^-$ calc for $C_{34}H_{61}N_2O_8Zn$: 691.2; [Zn(DD-DO2A)]: m/z (ES+) 689.7 $[M + H]^+$, calc. for $C_{36}H_{71}N_4O_4Zn$: 689.4; [Zn(DH-DO2A)]: m/z (ES+) 801.7 $[M + H]^+$, calc. for $C_{44}H_{87}N_4O_4Zn$: 801.6.

Liposomes preparation. Liposomes were prepared by using the conventional thin film hydration method.[32] Briefly, the lipid mixture (composed by DPPC, DSPE-PEG2000 and the amphiphilic Mn(II) or Zn(II) complexes, in molar ratio 85:5:10 or 75:5:20) was dissolved in chloroform (total lipid amount of 20 mg/mL). The organic solution was slowly evaporated to remove the solvent until a thin film was formed, that was afterward hydrated at 55°C with an isotonic HEPES/NaCl buffer (pH = 7.4). To evaluate the presence of the aqueous liposomes core, the hydration of the film was performed with an aqueous solution of the MRI contrast agent Gadoteridol (Scheme 1, 250 mM, isotonic) or with a solution of the water-soluble fluorescent dye carboxyfluorescein (20 mM + HEPES buffer until reaching isotonicity). Liposomes were obtained by extrusion (Lipex extruder, Northern Lipids Inc., Canada) through polycarbonate filters with pore diameter of 200 nm (2 times) and 100 nm (4 times). The final suspension of the nanovesicles was purified by exhaustive dialysis carried out at 4°C against the isotonic buffer. Mean hydrodynamic diameter and polydispersity (PDI) of the systems were determined by DLS (Dynamic Light Scattering, Zetasizer NanoZs, Malvern instruments, UK).

Cryo-TEM analysis. Cryo-transmission electron microscopy was employed to characterize size and shape of the obtained nanoparticles. Samples were vitrified on carbon-coated cryoTEM grids

with a vitrification robot (Vitrobot Mark III, FEI, Hillsboro, USA). Imaging was performed on a Tecnai 20 Sphera TEM instrument (FEI) equipped with a LaB6 filament (200 kV) and Gatan cryoholder (approximately -170°C) at 25000x magnification.

Relaxometric measurements. The magnetic field dependence of the water proton spin-lattice relaxation rates ($1/T_1$) for liposomes encapsulating paramagnetic Mn(II) complexes were measured (at 298K and 310 K) on a Stelar Spinmaster FFC-2000 fast-field cycling relaxometer, over a continuum range of field strengths (from 0.00024 to 0.25 T, corresponding to 0.01–10 MHz proton Larmor frequencies). Additional data points in the range 15–70 MHz were obtained on a BrukerWP80 NMR electromagnet adapted to variable-field measurements with a Stelar relaxometer. The temperature was controlled using a Stelar VTC-91 variable temperature unit equipped with a copper-constantan thermocouple (uncertainty of ±0.1 °C). The ^{1}H T_1 relaxation times were acquired by the standard inversion recovery method with typical 90°pulse width of 3.5 μs, using 16 experiments of 4 scans each. The T_1 reproducibility was within 5%. The exact concentration of Mn(II) was determined by the measurement of bulk magnetic susceptibility shifts of the *t*BuOH signal[31] or by inductively coupled plasma mass spectrometry (ICP-MS, Element-2, Thermo-Finnigan, Rodano (MI), Italy). Sample digestion was performed with concentrated HNO_3 (70%, 2 mL) under microwave heating at 160 °C for 20 min (Milestone MicroSYNTH Microwave lab station equipped with an optical fibre temperature control and an HPR-1000/6M six position high pressure reactor, Bergamo, Italy). The concentration of Gd(III) in the suspension of particles obtained from the hydration with gadoteridol and incorporated with the amphiphilic Zn(II) complexes was determined by ICP-MS after mineralization of the samples.

Results and discussion

The two hydrophobic chains of $M(HCDTA)^{2-}$, M(DD-DO2A), and M(DH-DO2A) (M = Mn(II) or Zn(II)), allowed the incorporation of the metal complexes in the lipid bilayer of liposomes, with the aim of improving the motional coupling between the paramagnetic complex and the nanoparticle. Liposomes were prepared by the conventional thin film hydration method starting from a lipid mixture composed by DPPC, DSPE-PEG2000 and the amphiphilic metal complex in molar ratio 85:5:10 or 75:5:20.

Table 1. Results of the DLS experiments for the particles incorporating the reported Mn(II) complexes.

Incorporated complex	mol.% MnL	d (nm)	PDI
$Mn(HCDTA)^{2-}$	10%	25.4	0.5
	20%	13.9	0.3
Mn(DD-DO2A)	10%	109.0	0.2
	20%	36.1*	0.9
Mn(DH-DO2A)	20%	124.0	0.1

* This size represented 99.8 % of the population. The remaining 0.2 % showed a diameter of 100 nm

Table 1 shows the values of the mean hydrodynamic diameter (d) and corresponding polydispersity index (PDI) values obtained by DLS for the nanoparticles incorporating the Mn(II) complexes. The results obtained indicate that the size may be dependent on both the type and the amount of the embedded complex. The hydrodynamic diameters of the samples formulated with the Mn(II) complex functionalized with the longer C_{16} chains (Mn(DH-DO2A)) were in the typical range (100-170 nm) displayed by conventional liposomes prepared according to the method based on the hydration of thin lipid film. Conversely, the incorporation of the Mn(II) complexes bearing the shorter C_{12} chains invariantly led to much smaller particles, regardless of the macrocyclic

Mn(DD-DO2A), or acyclic $Mn(HCDTA)^{2-}$ structure of the ligand. Furthermore, the size reduction was directly correlated to the percentage of complex incorporated in the particles, as clearly observable for $Mn(HCDTA)^{2-}$ and Mn(DD-DO2A) complexes. Polydispersity values paralleled the size effects, and larger size dispersions were generally observed for the smaller particles. The sample formulated with Mn(DD-DO2A) 20% contained a small percentage (0.2%) of a population of 100 nm (likely nanovesicular). For this reason, the following studies on this chelate were carried out using the 10% formulation. On the other hand, as the system formulated with Mn(DH-DO2A) 20% contained a single population of liposomes, it has been deemed irrelevant to investigate the 10% formulation.

In order to verify the vesicular properties of the nanoparticles, proton NMR relaxometry and electron microscopy experiments were carried out. The use of ^{1}H NMR relaxometry to confirm the presence of nanovesicles is based on the rational that only vesicular aggregates can entrap a paramagnetic water-soluble MRI contrast agent (here gadoteridol (Gd(HP-DO3A), HP-DO3A = 2,2',2''-[10-(2-hydroxypropyl)-1,4,7,10-tetraazacyclododecane-1,4,7-triyl]triacetate, Scheme 1) after the hydration of the lipid film and successive dialysis to remove the not encapsulated agent. Hence, the measurement of the longitudinal relaxation rate of the suspension containing the particles will support the presence of the paramagnetic species in the aqueous compartment of the nanovesicle, whereas for non-vesicular particles the relaxometric response will match that one of the diamagnetic sample. The presence of the entrapped agent can be also revealed by any analytical technique able to detect and quantify the metal (Gd(III) or Mn(II)) complex (*i.e.* ICP-MS), but relaxometric measurements can also provide useful information to assess the potential of the system to act as MRI reporter of drug release. In fact, the entrapment of a water-soluble paramagnetic agent in the aqueous core of a particle may quench the relaxivity depending on the

permeability of the membrane of the nanovesicle to water.[31] This phenomenon occurs when the exchange of the water protons of the vesicle cavity with the external compartment is slower than their NMR longitudinal relaxation rate (*i.e.* $R_1^{intralipo} > k_{ex}^{intralipo}$). This condition is favored by high $R_1^{intralipo}$ values, which can be achieved when the concentration of the entrapped agent is high (*i.e.* hundreds millimolar) and/or by low water permeability values of the vesicle membrane, which can be obtained formulating the system with phospholipids containing saturated fatty acids (typically derived from palmitic, C_{16}, or stearic, C_{18}, acids).[33, 34]

Table 2. Concentration of gadoteridol found in the nanoparticles formulated with the listed amphiphilic Zn(II)-complexes. Total amount of amphiphilic components in the formulation 20 mg/mL.

Incorporated complex	Encapsulated gadoteridol - mM
$Zn(HCDTA)^{2-}$ (20%)	0.01
$Zn(HCDTA)^{2-}$ (10%)	3.9
$Zn(DD\text{-}DO2A)^{2-}$ (10%)	5.9
$Zn(DH\text{-}DO2A)^{2-}$ (20%)	14.6

The experiments to verify the vesicular property of the nanoparticles were carried out hydrating the lipid thin film with a concentrated solution (250 mM) of the clinically approved agent gadoteridol. A total amount of 20 mg/mL of lipid material was used for all the samples and to avoid the interference between the two paramagnetic ions (Gd(III) and Mn(II)), the amphiphilic ligands were coordinated by the diamagnetic Zn(II) ion. The total concentration of gadoteridol found in the different formulations after washing out the non-encapsulated agent are reported in Table 2. The results show a progressive reduction in the loading of the hydrophilic compound that follows the order Zn(DH-DO2A) 20% > Zn(DD-DO2A) 10% > $Zn(HCDTA)^{2-}$ 10% >> $Zn(HCDTA)^{2-}$ 20%. Due to the almost negligible amount of gadoteridol, the particles formulated

with 20% of the linear $M(HCDTA)^{2-}$ complex appear fully non-vesicular. Moreover, the concentration of the entrapped gadoteridol in the other formulations varied considerably, positively correlating with particle size and negatively correlating with particle size dispersion (Table 1). This suggests that the amphiphilic chelates have a crucial role in determining the morphology of the phospholipid-based nanoparticles.

Figure 1 shows a panel of cryo-TEM images referring to some formulations examined in this work. The images clearly highlight the different morphologies displayed by the nanoparticles. Notably, the aggregates containing Zn(DH-DO2A) 20% showed the typical liposomal pattern. Liposomal structures are visible even in the sample formulated with 10 % of the macrocyclic complex Zn(DD-DO2A), but they are mixed with some well-contrasted rod-like structures.

The latter "nano-objects" predominated in the images obtained for the sample incorporating $Zn(HCDTA)^{2-}$, especially for the 20% formulation. The difference between the morphology of the two $Zn(HCDTA)^{2--}$-based aggregates is particularly clear in Figure 2. Besides the presence of these "black bars", the images emphasize the presence of much less contrasted spherical structures, whose diameter is very close to the length of the rods. This observation is an indication that $Zn(HCDTA)^{2-}$ samples is constituted by non-vesicular disk-shaped aggregates, whose abundance is proportional to the amount of metal complex in the formulation.

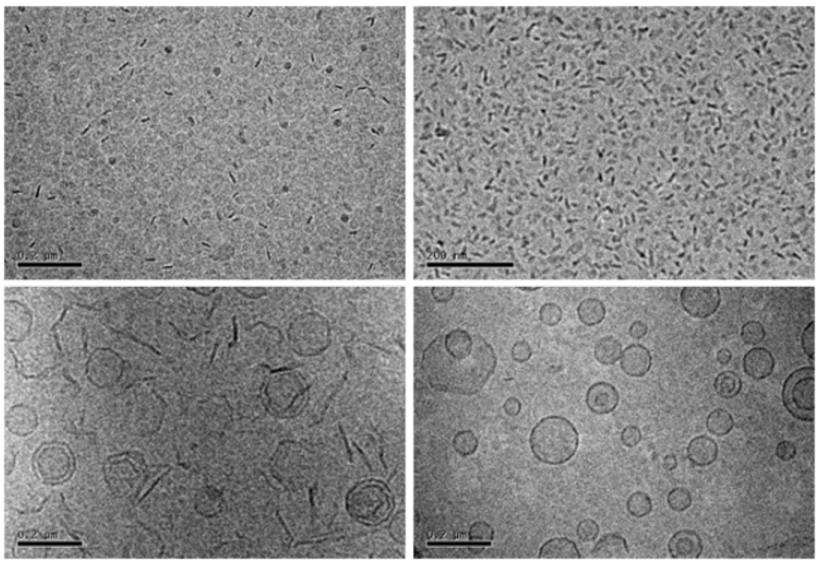

Figure 1. Cryo-TEM images of phospholipid-based nanoparticles entrapping: $Zn(HCDTA)^{2-}$ 10% (top left), $Zn(HCDTA)^{2-}$ 20% (top right), Zn(DD-DO2A) 10% (bottom left), and Zn(DH-DO2A) 20% (bottom right). Scale bar 200 nm.

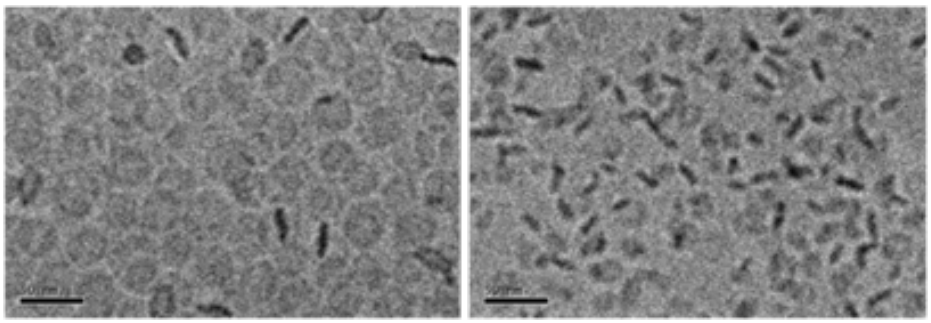

Figure 2. Expanded cryo-TEM images of phospholipid-based nanoparticles entrapping: $Zn(HCDTA)^{2-}$ 10 % (left) and $Zn(HCDTA)^{2-}$ 20 % (right). Scale bar 50 nm. (consider that the 10% sample entraps some gadoteridol).

Taken together, the results presented so far can be summarized as follows: it seems clear that the amphiphilic metal complexes that contain two short C_{12} aliphatic chains affect the size and the morphology of the corresponding self-aggregates. This effect is very evident for the formulations containing the acyclic $Zn(HCDTA)^{2-}$ complex in which the formation of non-vesicular aggregates was already observed in the 10% formulations. Contrarily, the formulation containing 10% of the macrocyclic Mn(DD-DO2A) complex was mostly composed of liposomes, with only a small fraction of non-vesicular aggregates (Figure 1, bottom left). Hence, the switch from nanovesicular particles to non-vesicular aggregates was accompanied by a significant and progressive reduction of the mean hydrodynamic diameter of the particles and an increase in the overall polydispersion

of the system. Interestingly, the progressive reduction in the fraction of vesicular nanoparticles inferred from cryo-TEM experiments followed the same order (M(DH-DO2A) > M(DD-DO2A) > M(HCDTA)$^{2-}$) obtained from the measurement of the amount of gadoteridol entrapped in the aggregates (Table 2), thus outlining the relevance of this methodology to provide an indirect access to the morphology distribution of the samples.

The size of the self-assembled soft phospholipid-based nanoparticles is determined by several factors, among which the molecular shape and the hydrophobic/hydrophilic ratio of the amphiphilic components play a relevant role because they define the curvature of the bilayer (in the case of vesicular systems) or the tendency to assume different shapes (spherical, disks, rods) for micellar aggregates.[35-37] Generally, cylinder-shaped molecules (like C_{16}-C_{18} phospholipids) prefer to self-assemble in bilayer, thus forming vesicles, whereas more conical molecules (*e.g.* phospholipids with short chains), with a predominance of the hydrophilic portion, prefer to self-aggregate in micelles.[38] Therefore, it is likely that the results herein reported can be rationalized in terms of a change in shape and hydrophobic/hydrophilic ratio between the complexes bearing C_{12}- and C_{16} lipophilic tails.

On this basis, the different behavior observed for the two coordination cages (acyclic EDTA *vs* macrocyclic DO2A) could be primarily related to the overall shape of the two amphiphiles, which is certainly affected by the structural features of the ligands, especially for the different anchoring position of the aliphatic tails on the ligand skeleton. Likely, for a given alkyl chain length, the increased distance between the anchoring points in case of the DO2A-like cage favors a cylindric molecular shape that, in turn, facilitates the formation of vesicular structures *versus* micellar ones. What remains still important to elucidate is the real structure of the aggregates that do not behave (and do not appear) as conventional liposomes. Though this task is rather challenging, the literature

provides several publications where cryo-TEM images similar to those obtained in this work were observed and explained based on a liposome-to-micelle switch.

For instance, Johnsson and co-workers reported a series of cryo-TEM images of aggregates based on DPPC and showed that the transition from liposomes to a micellar phase, consisting of small spherical particles, occurred *via* the formation of discoidal micelles.[39] Moreover, it was reported that the size of such disks decreased upon increasing the amount of DPPE-PEG (more hydrophilic phospholipid) in the formulation. A typical example of these discoidal structures is represented by bicelles (bilayered micelles) that form when phospholipids with long aliphatic chain (C_{16}-C_{18} in length) are properly mixed with amphiphiles with shorter chains (typically C_6). Bicelles are described as soft aggregates that do not entrap water and, in electron microscopy, are detected by the presence of edge-on (black bars) and face-on (low intense circular objects) structures.[40] It is noteworthy that the cryo-TEM images acquired on the samples containing HCDTA-based complexes displayed objects with a morphology very similar to that one reported for bicelles.[40] Nevertheless, it is very important to outline that the aggregates containing 10% of $Zn(HCDTA)^{2-}$ (as well as those containing 20% of Zn(DD-DO2A)) are able to encapsulate gadoteridol (in case of $Zn(HCDTA)^{2-}$ also the water-soluble fluorescent dye carboxyfluorescein, see Supporting Information), thereby clearly indicating the presence of a fraction of aggregates having vesicular properties. A further support to the vesicular nature of the aggregates entrapping gadoteridol can be gained by comparing the relaxivity values measured before and after the chemical degradation of the aggregates with the detergent Triton X-100. If the relaxivity of the intact system is quenched, then the degradation will result in a relaxivity enhancement, and this occurred for Zn(DH-DO2A) 20% (enhancement 1240%) and $Zn(HCDTA)^{2-}$ 10% (enhancement 27%) (Supporting Information). Interestingly, the remaining sample with vesicular characteristics,

Zn(DD-DO2A) 20%, did not display any relaxivity enhancement, likely due to the very low fraction of vesicular aggregates or to the occurrence of a not quenching condition (reduced $R_1^{intralipo}$ and/or increased $k_{ex}^{intralipo}$) for that specific sample.

The whole set of collected data may be interpreted by two hypotheses, both based on the observation that the metal complexes have a predominant role to promote the switch from vesicles/liposomes to bicelles-like aggregates: a) the bicelles disks are not perfectly "sealed" and some water can be entrapped in the aggregates that would behave as a sort of "vesicular bicelles", and/or b) a fraction of vesicles/liposomes is present in the suspension together with the non-vesicular aggregates, thus contributing to the overall entrapment of the water-soluble probes. All the experiments performed with the aim of assessing the morphologic properties of the aggregates (DLS, cryo-TEM, addition of hydrophilic probes) definitely support the second hypothesis.

In order to assess the MRI potential of the systems under investigation, the samples were subjected to a ^{1}H NMR relaxometric study. Firstly, the relaxivity of the five samples was measured at different temperatures (298 K and 310 K) and magnetic field strengths (0.5 T, 1 T, and 1.5 T) (Figure 3).

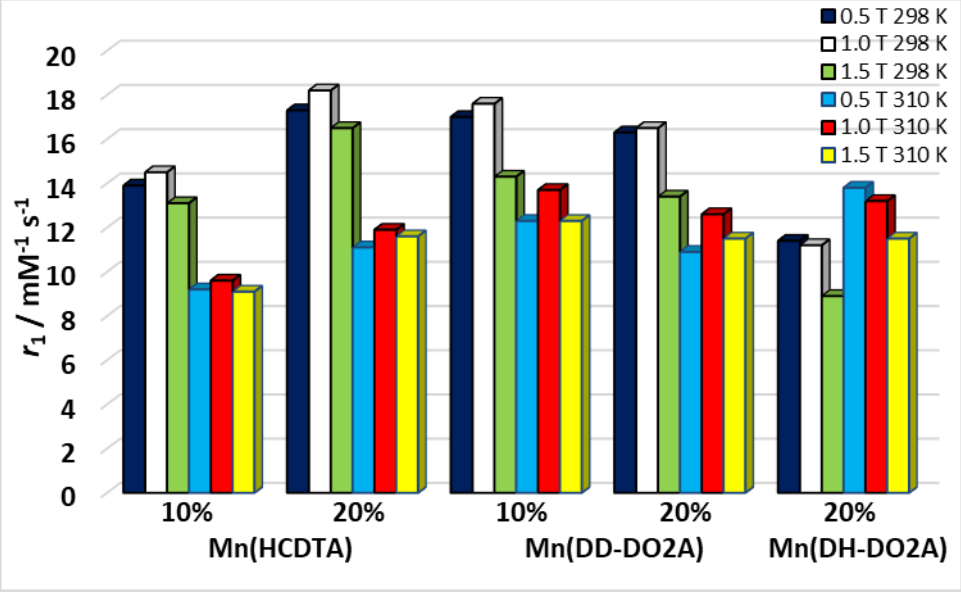

Figure 3. Relaxivity values (mM^{-1} s^{-1}) of phospholipid-based nanoparticles incorporating the different Mn(II) complexes as a function of temperature and magnetic field strength.

When compared with the relaxivities reported for amphiphilic Gd(III) complexes incorporated in conventional nanovesicular particles,[6] the obtained r_1 values are rather low, most likely due to the weaker paramagnetic effect of the Mn(II) ion associated with its lower magnetic moment. Furthermore, at first glance, whereas the relaxivities at 0.5 T and 1 T are rather similar, the values measured at 1.5 T are lower. Interesting and useful information is obtained from the effect of temperature on r_1. While in $Mn(HCDTA)^{2-}$ and Mn(DD-DO2A)-based particles the relaxivity decreases by increasing the temperature to indicate the occurrence of a fast exchange condition of the bound water molecule, Mn(DH-DO2A) behaves in an opposite way.

More accurate and detailed information can be extracted from the field-dependence of the longitudinal relaxation rate using fast field-cycling relaxometry (FFC-NMR). The acquisition of Nuclear Magnetic Relaxation Dispersion (NMRD) profiles of aqueous solutions of paramagnetic metal chelates and their analysis based on the established theory of paramagnetic relaxation allow obtaining reliable estimation of several structural, electronic and dynamic parameters. These include the number (q) of water molecules in the inner coordination sphere, their distance (r) from the paramagnetic center, the relationship between electronic relaxation (Δ^2 and τ_V) and structural properties of the complex, the exchange lifetime (τ_M) of the coordinated water molecule(s) and the overall molecular tumbling time (τ_R). Of course, only in the case of systems with a well-defined composition does this type of analysis have a precise physical meaning. Therefore, based on what has been previously discussed, we have restricted the investigation to Mn(DD-DO2A) (20%) whose vesicular nature is demonstrated and to $Mn(HCDTA)^{2-}$ (20%) which is present in solution

in the form of bicellar aggregates. The ^{1}H NMRD profiles of all the nanosystems were measured at 298 and 310 K over the frequency range 0.01 – 70 MHz (Figure 4 and SI).

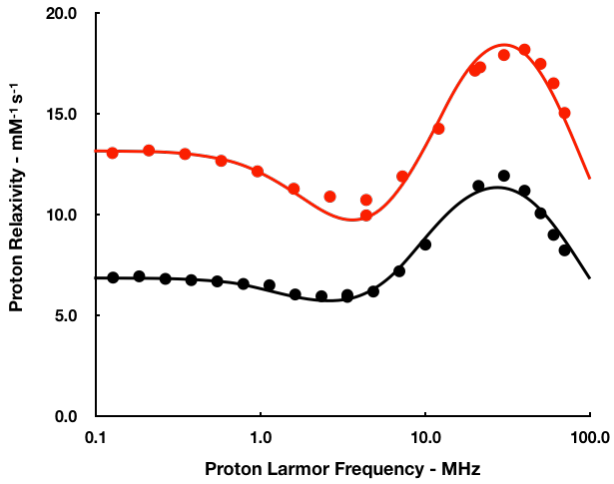

Figure 4. NMRD profiles (at 298 K) of the liposomes incorporating Mn(DH-DO2A) 20% (black) and Mn(HCDTA) 20% (red).

Despite some significant differences, the profiles have a rather similar general trend, with the characteristic shape of macromolecular systems with a reduced rotational tumbling rate. We can identify four distinct sections in the NMRD profiles: a) a region of constant relaxivity at low fields (~ 0.01-0.8 MHz); b) a smooth and little pronounced dispersion in the range 1-4 MHz; c) a relatively narrow peak centered about 20-30 MHz; d) a steep decrease of r_1 at higher frequencies.

Mn(DH-DO2A) 20%. This system, when Zn replaced Mn, showed the highest internalization of gadoteridol, thus indicating the liposomal nature of the nanoparticles, as confirmed also by the cryo-TEM images. The best-fit procedure has been carried out using the well-established Solomon-Bloembergen-Morgan relaxation model (SBM)[41] coupled to the Lipari–Szabo approach[42] for the description of the rotational dynamics. This latter allows the separation of the local molecular rotation of the chelates (characterized by the correlation time τ_{RL}) from the global

tumbling motion of the nanoparticle (τ_{RG}). The degree of correlation between the two types of motion is described by the order parameter S^2 whose value falls between 0 (entirely uncorrelated motions) and 1 (complete motional coupling). In addition, we considered not only the contribution to relaxivity arising from the metal centers on the external leaflet of the bilayer, but also the relaxation generated by the metal complexes pointing inward to the aqueous core of the aggregate.[30] According to this model, bulk water protons receive a contribution to relaxivity from the water protons in the inner core of the vesicles, proportional to the volume fraction of the intraliposomal pool and dependent on both the relaxation time of the protons entrapped in the liposomes and their residence lifetime in the vesicles. In turn, this residence lifetime depends on the water permeability of the liposome bilayer (P_W) and the vesicle size.[30] In the least-square fitting analysis, some of the parameters were fixed. In particular, standard values were assigned to the distance of closest approach between the paramagnetic metal ion and bulk water protons, a, and to the relative diffusion coefficient of solute and solvent, D. In addition, the number (q) of bound water molecules, their distance (r_{Mn-H}) from the metal center and their rate of chemical exchange with bulk water ($k_{ex} = 1/\tau_M$) were fixed to the values reported for the same complex aggregated in mixed micelles (*i.e.* micelles containing 50% of the amphiphilic chelate and 50% of pegylated phospholipids).[24] The fractional value of the hydration number ($q = 0.87$) was used in accordance with what was previously determined for Mn(1,4-DO2A)[25] and Mn(DB-DO2A) (DB-DO2A = 1,4-dibutyl-DO2A).[24] The calculated parameters are reported in Table 3 and compared to the values obtained for the same complex incorporated in mixed micelles.[24] Apart from the parameters describing the electronic relaxation, Δ^2 (trace of the squared zero-field splitting, ZFS, tensor) and τ_V (correlation time for the modulation of the transient ZFS), which have a very limited physical meaning for slowly tumbling systems, the main factor governing the relaxivity and limiting its

enhancement appears to be the flexibility of the pendant aliphatic chain. This is evidenced by the significant difference between the values of the local and global rotational correlation times. The S^2 parameter also assumes a value that indicates a poor motional coupling between local and global rotation. The permeability of the vesicle bilayer to water obtained from the analysis is slightly lower than the values reported for similar liposomes incorporated with macrocyclic lanthanide complexes,[31] thus suggesting that the insertion of saturated alkyl chains has a little effect on the ability of water to cross the bilayer. It is worth noting that fixing the value of q at 0.87 (model I in Table 3) does not significantly affect the results of the analysis. In fact, assuming for q a value equal to 1 (model II) the values of the other parameters vary only marginally. The values are also quite similar to those of the mixed micelles reported previously,[24] apart from the value of τ_{RG} which is closely related to the size of the systems.

Table 3. Selected best fit parameters (298 K) obtained from the analysis of the $1/T_1$ NMRD profiles of Mn(DH-DO2A) 20% and Mn(HCDTA) 20%.[a]

	Micelles[b]	Liposomes (model I)	Liposomes (model II)	Mixed micelles[b]	Bicelles (this work)
	Mn(DH-DO2A) 20%			**Mn(HCDTA) 20%**	
Δ^2	1.6	1.6	1.72	1.8	2.1
τ_V / ps	36.0	54.5	53.5	33.0	44.8
τ_{RL} / ps	81	96.3	82.1	102	180
τ_{RG} / ns	9	49.2	54.5	3.2	5.0
S^2	0.28	0.44	0.37	0.38	0.30
τ_M / ns[c]	2.9	2.9	2.9	3.2	3.2
P_W / $\times 10^{-5}$ cm s^{-1}	/	0.6	0.51	--	--
q[c]	0.87	0.87	1	1	1

[a] r_{MnH}, a and ^{298}D were fixed in the fitting procedure to 2.83 Å, 3.6 Å and 2.3×10^{-5} cm^2 s^{-1}, respectively; [b] from reference 22; [c] fixed during the fitting procedure.

Mn(HCDTA) 20%. This system, when Zn replaced Mn, did not entrap gadoteridol. Therefore, we can reasonably assume that the complex is present only in the form of micellar aggregates, without the presence of vesicular particles. This hypothesis is well supported by the results of cryo-TEM. The fitting procedure is completely analogous to the previous case, except for the absence of the P_W parameter as the internal aqueous core is missing. In other words, the metal complexes interact only with the bulk water molecules. Therefore, as before, the parameters a, D, q, $r_{Mn\text{-}H}$ and τ_M were fixed to standard values or to those used in a previous analysis in which the complexes were embedded in mixed micelles.[24] The result of the best-fit is quite good. The NMRD profile (Figure 4) is well reproduced using the parameters reported in Table 3. As expected, given their relative size, the τ_{RG} value is much lower than in the previous case but this seems to have a limited impact on the relaxivity. In fact, far more important is the role played by local motions (τ_{RL}), as already noted. The value of this parameter is greater for $Mn(HCDTA)^{2-}$ than for Mn(DH-DO2A) and consequently the relaxivity is higher along the entire frequency range explored. Even if we treat Δ^2 and τ_V only as fitting parameters, without giving them a precise meaning, the very similar values obtained for the two complexes in the two macromolecular systems provide support to the validity of the analysis results.

In spite of their remarkable differences in size and morphology, the r_1 values of the aggregates containing Mn(DD-DO2A) 20% and Mn(HCDTA) 20% did not significantly change with respect to the corresponding preparation containing 10% of the two chelates (Figure 3 and SI). This finding can be explained by considering that the water permeability of the vesicular bilayers incorporating these complexes marginally limit, or it does not limit at all, the relaxivity and, therefore, vesicular and non-vesicular aggregates could have similar relaxivities. However, it has to be noted that the relaxivity normalized to the concentration of the particles (and not to the paramagnetic complex)

depends on the number of paramagnetic complexes incorporated in the aggregate. Therefore, it is expected that the sensitivity of the MRI detection for the intact particles loaded with 20% of Mn(II) complex is certainly higher than the formulation containing 10% of the chelate.

Conclusions

In summary, the results herein reported highlight, for the first time, the relevance of the structural properties of amphiphilic paramagnetic Mn(II)-complexes to control size and morphology of phospholipid-based self-assembling nanoaggregates. It is likely that the polydispersion of such systems may be optimized through a fine-tuning of the amount of a given complex added in the formulation. If this approach will succeed, it will be possible to prepare an almost monodisperse suspension of vesicular liposomes or not vesicular bicelles. Each one of these nanoparticles will exhibit different properties not only in terms of biodistribution and excretion, but also for the generation of MRI contrast that will allow the in vivo guidance of the delivery and release of a given drug in a pathological region. Another important finding of this work is the observation of the remarkable effect played by the nature of the metal complex on the water permeability of the soft aggregates that can significantly affect the capability of the system to generate MRI contrast. Finally, we may assume that the lower toxicity profile of Mn(II) complexes with respect to Gd(III)-based agents and the good thermodynamic stability and kinetic inertness of Mn(1,4-DO2A) chelates could pave the way to promising further application as MRI contrast or theranostic agents.

ASSOCIATED CONTENT

Supporting Information. Analytical data on formulation, size, relaxivity and concentration of the various lipidic nanoparticles. NMRD profiles and 298 and 310 K of all Mn(II) nanosystems. Cryo-TEM images of Zn(II)-chelates containing nanosystems.

AUTHOR INFORMATION

Corresponding Authors

E-mail: lorenzo.tei@uniupo.it

E-mail: enzo.terreno@unito.it

Present Addresses

† Gilberto Mulas, Porto Conte Ricerche, Strada Provinciale 55, Km 8,400, 07041 Tramariglio, Alghero, Italy

Author Contributions

The manuscript was written through contributions of all authors. All authors have given approval to the final version of the manuscript. ‡ G.A.R. and G.M. equal contribution.

ACKNOWLEDGMENT

C.F.G.C.G. thanks FCT-Portugal (Portuguese Foundation for Science and Technology) and FEDER – European Regional Development Fund through the COMPETE Programme (Operational Programme for Competitiveness) for funding (UID/QUI/00313/2013 and PEst-OE/QUI/UI0313/2014). C.F.G.C.G also acknowledges the financial support of the EU COST Action COST CA15209 (EuRELAX) for a Short Term Scientific Mission to Torino, Italy.

REFERENCES

(1) Terreno, E; Delli Castelli, D; Viale, A; Aime, S. Challenges for molecular magnetic resonance imaging. *Chem. Rev.* **2010**, *110*, 3019-3042.

(2) Terreno, E; Uggeri, F; Aime, S. Image guided therapy: the advent of theranostic agents. *J Control. Rel.* **2012**, *161*, 328-337.

(3) Koo, H; Huh, M. S.; Sun, I. C.; Yuk, S. H.; Choi, K.; Kim, K.; Kwon, I. C. In vivo targeted delivery of nanoparticles for theranosis. *Acc. Chem. Res.* **2011**, *44*, 1018-1028.

(4) Grimaldi, N; Andrade, F.; Segovia, N.; Ferrer-Tasies, L.; Sala, S.; Veciana, J.; Ventosa, N.; Lipid-based nanovesicles for nanomedicine. *Chem. Soc. Rev.* **2016**, *45*, 6520-6545.

(5) Aime, S; Delli Castelli, D.; Geninatti Crich, S.; Gianolio, S.; Terreno, E. Pushing the sensitivity envelope of lanthanide-based Magnetic Resonance Imaging (MRI) contrast agents for molecular imaging applications. *Acc. Chem. Res.* **2009**, *42*, 822-831.

(6) Mulder, W. J.; Strijkers, G. J.; van Tilborg, G. A.; Griffioen, A. W.; Nicolay K. Lipid-based nanoparticles for contrast-enhanced MRI and molecular imaging. *NMR Biomed.* **2006**, *19*, 142-164.

(7) Botta, M.; Tei, L. Relaxivity enhancement in macromolecular and nanosized Gd^{III}-based MRI contrast agents. *Eur. J. Inorg. Chem.* **2012**, *12*, 1945-1960.

(8) Langereis, S.; Geelen, T.; Grull, H.; Strijkers, G. J.; Nicolay, K. Paramagnetic liposomes for molecular MRI and MRI-guided drug delivery. *NMR Biomed*. **2013**, *26*, 728-744.

(9) Grange, C.; Geninatti Crich, S.; Esposito, G.; Alberti, D.; Tei, L.; Bussolati, B.; Aime A.; Camussi, G. Combined Delivery and Magnetic Resonance Imaging of Neural Cell Adhesion Molecule–Targeted Doxorubicin- Containing Liposomes in Experimentally Induced Kaposi's Sarcoma. *Cancer Res*. **2010**, *70*, 2180-2190.

(10) Terreno, E.; Delli Castelli, D.; Cabella, C.; Dastrù, W.; Sanino, A.; Stancanello, J.; Tei, L.; Aime, S. Paramagnetic Liposomes as Innovative Contrast Agents for Magnetic Resonance (MR) Molecular Imaging Applications. *Chem. Biodiversity* **2008**, *5*, 1901-1912.

(11) Filippi, M.; Catanzaro, V.; Patrucco, D.; Botta, M.; Tei, L.; Terreno, E. First in vivo MRI study on theranostic dendrimersomes, *J. Control. Release*, **2017**, *248*, 45-52.

(12) Yang, L.; Krefting, I.; Gorovets, A.; Marzella, L.; Kaiser, J.; Boucher, R.; Rieves, D. Nephrogenic systemic fibrosis and class labeling of gadolinium-based contrast agents by the Food and Drug Administration. *Radiology* **2012**, *265*, 248-253.

(13) Guo, B. J.; Yang, Z. L.; Zhang, L. J. Gadolinium Deposition in Brain: Current Scientific Evidence and Future Perspectives. *Front Mol Neurosci*. **2018**, *11*:335.

(14) Drahoš, B.; Lukeš, I.; Tóth, É. Manganese (II) complexes as potential contrast agents for MRI. *Eur. J. Inorg. Chem*. **2012**, *12*, 1975-1986.

(15) Botta, M.; Carniato, F.; Esteban-Gomez, D.; Platas-Iglesias, C.; Tei, L. Mn(II) compounds as an alternative to Gd-based MRI probes, *Future Med. Chem*. **2019**, *11*, 1461-1483.

(16) Rolla, G. A.; Tei, L.; Fekete, M.; Arena, F.; Gianolio, E.; Botta, M. Responsive Mn(II) complexes for potential applications in diagnostic Magnetic Resonance Imaging. *Bioorg. Med. Chem.* **2011**, *19*, 1115-1122.

(17) Wang, J.; Wang, H.; Ramsay, I. A.; Erstad, D. J.; Fuchs, B. C.; Tanabe, K. K.; Caravan, P.; Gale, E. M. Manganese-Based Contrast Agents for Magnetic Resonance Imaging of Liver Tumors: Structure-Activity Relationships and Lead Candidate Evaluation. *J. Med. Chem.* **2018**, *61*, 8811-8824.

(18) Regge, D.; Cirillo, S.; Macera, A.; Galatola, G. Mangafodipir trisodium: review of its use as an injectable contrast medium for magnetic resonance imaging. *Reports in Medical Imaging* **2009**, *2*, 55–68.

(19) Bertin, A.; Michou-Gallani, A.I.; Gallani, J.L.; Felder-Flesch, D. In vitro neurotoxicity of magnetic resonance imaging (MRI) contrast agents: influence of the molecular structure and paramagnetic ion. *Toxicol. In Vitro* **2010**, *24*, 1386-1394.

(20) Viglianti, B. L.; Ponce, A. N.; Michelich, C. R.; Yu, D.; Abraham, S. A.; Sanders, L.; Yarmolenko, P. S.; Schroeder, T.; MacFall, J. R.; Barboriak, D. P.; Colvin, O. M.; Bally, M. B.; Dewhirst, M. W. Chemodosimetry of in vivo tumor liposomal drug concentration using MRI. *Magn. Reson. Med.* **2006**, *56*, 1011-1018.

(21) Yeo, S. Y.; de Smet, M.; Langereis, S.; Vander Elst, L.; Muller, R. N.; Grüll, H. Temperature-sensitive paramagnetic liposomes for image-guided drug delivery: Mn^{2+} versus [Gd(HPDO3A)(H_2O)]. *Biochim. Biophys. Acta*, **2014**, *1838*, 2807-2816.

(22) Zhao, X.; Zhuo, R.; Lu, Z.; Liu, W. Synthesis, characterization and relaxivity of amphiphilic chelates of DTPA derivates with Gd^{III}, Yb^{III} and Mn^{II}. *Polyhedron* **1997**, *16*, 2755-2759.

(23) Schwendener, R. A.; Wüthrich, R.; Duewell, S.; Wehrli, E.; von Schulthess, G. K. A pharmacokinetic and MRI study of unilamellar gadolinium-, manganese-, and iron-DTPA-stearate liposomes as organ-specific contrast agents. *Invest Radiol*. **1990**, *25*, 922-932.

(24) Rolla, G. A.; De Biasio, V.; Giovenzana, G. B.; Botta, M.; Tei, L. Supramolecular assemblies based on amphiphilic Mn^{2+}-complexes as high relaxivity MRI probes. *Dalton Trans*. **2018**, *47*, 10660-10670.

(25) Kálmán, F. K.; Tircsó, G. Kinetic inertness of the Mn^{2+} complexes formed with AAZTA and some open-chain EDTA derivatives, *Inorg Chem*. **2012**, *51*, 10065-10067.

(26) Garda, Z.; Forgács, A; Do, Q. N.; Kálmán, F. K.; Timári, S.; Baranyai, Z.; Tei, L.; Tóth, I.; Kovács, Z.; Tircsó, G. Physico-chemical properties of Mn^{II} complexes formed with cis- and trans-DO2A: thermodynamic, electrochemical and kinetic studies. *J Inorg Biochem*. **2016**, *163*, 206-213.

(27) Rolla, G. A.; Platas-Iglesias, C.; Botta, M.; Tei, L.; Helm, L. ^{1}H and ^{17}O NMR Relaxometric and Computational Study on Macrocyclic Mn(II) Complexes. *Inorg. Chem*. **2013**, *52*, 3268-3279.

(28) Filippi, M.; Remotti, D.; Botta, M.; Terreno, E.; Tei, L. GdDOTAGA$(C_{18})_2$: an efficient amphiphilic Gd(III) chelate for the preparation of self-assembled high relaxivity MRI nanoprobes. *Chem Commun*. **2015**, *51*, 17455-17458.

(29) Kielar, F.; Tei, L.; Terreno, E.; Botta, M. Large relaxivity enhancement of paramagnetic lipid nanoparticles by restricting the local motions of the Gd^{III} chelates. *J. Am. Chem. Soc.* **2010**, *132*, 7836-7837.

(30) Cittadino, E.; Botta, M.; Tei, L.; Kielar, F.; Stefania, R.; Chiavazza, E.; Aime, S.; Terreno, E. In vivo magnetic resonance imaging detection of paramagnetic liposomes loaded with amphiphilic Gadolinium (III) complexes: impact of molecular structure on relaxivity and excretion efficiency. *Chempluschem* **2013**, *78*, 712-722.

(31) Corsi, D. M.; Platas-Iglesias, C.; van Bekkum, H.; Peters, J. A. Determination of paramagnetic lanthanide(III) concentrations from bulk magnetic susceptibility shifts in NMR spectra. *Magn. Res. Chem.* **2001**, *39*, 723-726.

(32) Delli Castelli, D.; Terreno, E.; Cabella, C.; Chaabane, L.; Lanzardo, S.; Tei, L.; Visigalli, M.; Aime, S. Evidence for in vivo macrophage mediated tumor uptake of paramagnetic/fluorescent liposomes. *NMR Biomed.* **2009**, *22*, 1084-1092.

(33) Terreno, E.; Sanino, A.; Carrera, C.; Delli Castelli, D.; Giovenzana, G. B.; Lombardi, A.; Mazzon, R.; Milone, L.; Visigalli, M.; Aime, S. Determination of water permeability of paramagnetic liposomes of interest in MRI field. *J. Inorg. Biochem.* **2008**, *102*, 1112-1119.

(34) Koenig, S. H.; Ahkong, Q. F.; Brown, R. D.; Lafleur, M.; Spiller, M.; Unger, E.; Tilcock, C. Permeability of liposomal membranes to water: results from the magnetic field dependence of T1 of solvent protons in suspensions of vesicles with entrapped paramagnetic ions. *Magn. Reson. Med.* **1992**, *23*, 275-286.

(35) Chen, M.; McDaniel, J.; MacKay, J. A.; Chilkoti, A. Nanoscale self-assembly for delivery of therapeutics and imaging agents. *Technol. Innov.* **2011**, *13*, 5-25.

(36) Israelachvili, J. N. Self-assembling structures and biological systems, part III in *Intermolecular and surface forces*. Academic Press, Great Britain, **2011**.

(37) Beck, P.; Liebi, M.; Kohlbrecher, J.; Ishikawa, T.; Rüegger, H.; Fischer, P.; Walde, P.; Windhab, E. Novel type of bicellar disks from a mixture of DMPC and DMPE-DTPA with complexed lanthanides. *Langmuir* **2010**, *26*, 5382-5387.

(38) Alberts, B.; Johnson, A.; Lewis, J.; Raff, M.; Roberts, K.; Walter, P. The lipid bilayer in Molecular Biology of the Cell. Garland Science; USA, **2002**.

(39) Johnsson, M.; Edwards, K. Liposomes, disks, and spherical micelles: Aggregates structure in mixtures of gel phase phosphatidylcholines and poly(ethylene glycol)-phospholipids. *Biophys. J.* **2003**, *85*, 3839-3847.

(40) Rodríguez, G.; Soria, G.; Coll, E.; Rubio, L.; Barbosa-Barros, L.; López-Iglesias, C.; Planas, A. N.; Estelrich, J.; de la Maza, A.; López, O. Bicosomes: Bicelles in dilute systems. *Biophys. J.* **2010**, 99, 480-488.

(41) Bloembergen, N.; and Morgan, L. O. Proton relaxation times in paramagnetic solutions. Effects of electron spin relaxation. *J. Chem. Phys.* **1961**, *34*, 842–850.

(42) Lipari, G.; Szabo, A. Model-free approach to the interpretation of nuclear magnetic resonance relaxation in macromolecules. 2. Analysis of experimental results. *J. Am. Chem. Soc.* **1982**, *104*, 4560–4570.

SYNOPSIS

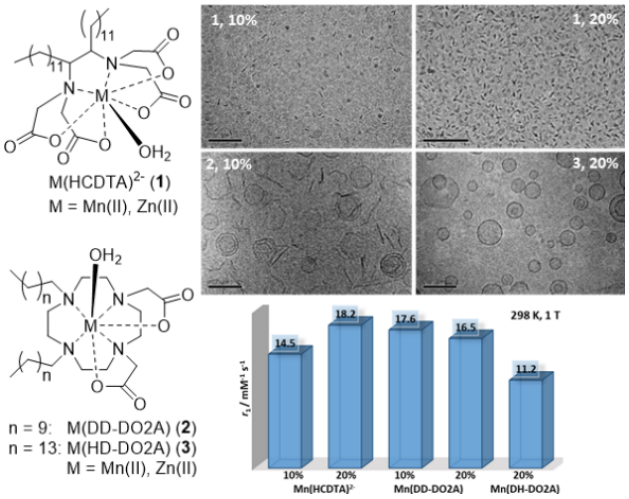
M(HCDTA)2- (1)
M = Mn(II), Zn(II)
n = 9: M(DD-DO2A) (2)
n = 13: M(HD-DO2A) (3)
M = Mn(II), Zn(II)
1, 10%
1, 20%
2, 10%
3, 20%
298 K, 1 T
r1 / mM-1 s-1
14.5
18.2
17.6
16.5
11.2
10%
20%
10%
20%
20%
Mn(HCDTA)2-
Mn(DD-DO2A)
Mn(DH-DO2A)